two carbamide ester groups. In contrast, the presence of four hydroxymethyl and two carbamide ester groups, and therefore a total of six hydrogen bond donor and acceptor functionalities, is considered to be less favorable. Our results suggest a limit on the number of hydrogen bond donor and acceptor groups, at least for this first series of symmetric modulators, and therefore provide an important contribution to the discussion on the role of hydrogen bonding with respect to activity. A comparison of the concentrations required for sufficient inhibitory activity (< 3 μM) and the CC_{50} values for the cyctotoxicity of **6b** and **6c** (> 93 and 125 μM, respectively), obtained from MTT assays[16] for the determination of lactate dehydrogenase (LDH) activity in metabolically active normal cells (MT-4), makes clear that the novel MDR modulators evoke convincing inhibitory activities at concentrations below those causing cytotoxic effects.

In conclusion, hydroxymethyl-substituted 3,9-diazatetraasteranes represent an independent class of novel MDR modulators that show activity at concentrations below cytotoxic levels. A highly interesting characteristic of these compounds is the rigidly symmetric form, which, owing to the extraordinary effect on the target structure, could be a reflection of the composition of the molecular pump or the potential bonding region, whose structure is as yet unknown. The goal of further work is to examine this "symmetry hypothesis" through the synthesis and investigation of unsymmetrical compounds. In order to estimate the clinical potential experiments are planned on additional resistant cell lines, whose MDR is based on the expression of molecular pumps other than the P-GP.

Received: March 7, 2002
Revised: July 5, 2002 [Z18849]

[1] D. A. Dougherty, H. A. Lester, *Angew. Chem.* **1998**, *110*, 2463 – 2466; *Angew. Chem. Int. Ed.* **1998**, *37*, 2329 – 2331.
[2] D. Rees, A. J. Chirino, K.-H. Kim, H. Komiya in *Membrane Protein Structure* (Ed.: S. H. White), Oxford University Press, New York, **1994**, pp. 1 – 26.
[3] a) R. L. Juliano, V. Ling, *Biochim. Biophys. Acta* **1976**, *455*, 152 – 162; b) M. M. Gottesmann, I. Pastan, *Annu. Rev. Biochem.* **1993**, *62*, 385 – 427; c) K. C. Almquist, D. W. Loe, D. R. Hipfner, J. E. Mackie, S. P. Cole, R. G. Deeley, *Cancer Res.* **1995**, *55*, 102 – 110.
[4] R. Preiss, *Int. J. Clin. Pharmacol. Therapeut.* **1998**, *36*, 3 – 8.
[5] a) T. Tsuruo, H. Iida, S. Tsukagoshi, Y. Sakurai, *Cancer Res.* **1982**, *41*, 1967 – 1972; b) N. J. Chao, M. Aihara, K. G. Blume, B. I. Sikic, *Exp. Hematol.* **1990**, *18*, 1193 – 1198; c) J. S. Kukl, B. I. Sikic, K. G. Blume, N. J. Chao, *Exp. Hematol.* **1992**, *20*, 1048 – 1054.
[6] a) H. Nawrath, M. Raschack, *J. Pharmacol. Exp. Ther.* **1987**, *242*, 1090 – 1097; b) R. Pirker, D. J. Fitzgerald, M. Raschack, Z. Frank, M. C. Willingham, I. Pastan, *Cancer Res.* **1989**, *49*, 4791 – 4795; c) T. Watanabe, M. Naito, T. Oh-hara, Y. Itoh, D. Cohen, T. Tsuruo, *Jpn. J. Cancer Res.* **1996**, *87*, 184 – 193.
[7] A. Hilgeroth, U. Baumeister, *Angew. Chem.* **2000**, *112*, 588 – 590; *Angew. Chem. Int. Ed.* **2000**, *39*, 576 – 578.
[8] a) D. Kessel, *Cancer Commun.* **1989**, *1*, 145 – 149; b) J. L. Weaver, D. Szabo, P. S. Pine, M. M. Gottesmann, S. Goldberg, A. Aszalos, *Int. J. Cancer* **1993**, *54*, 456 – 461; c) D. Sharples, G. Hajos, Z. Riedl, D. Csanyi, J. Molnar, D. Szabo, *Arch. Pharm. Pharm. Med. Chem.* **2001**, *334*, 269 – 274.
[9] a) H. L. Pearce, M. A. Winter, W. T. Beck, *Adv. Enzyme Regul.* **1990**, *30*, 357 – 373.
[10] G. Ecker, M. Huber, D. Schmidt, P. Chiba, *Mol. Pharmacol.* **1999**, *56*, 791 – 796.
[11] A. Seelig, E. Landwojtowicz, *Eur. J. Pharm. Sci.* **2000**, *12*, 31 – 40.
[12] A. Hilgeroth, A. Billich, *Arch. Pharm. Pharm. Med. Chem.* **1999**, *332*, 380 – 384.
[13] A. Seelig, L. Blatter, F. Wohnsland, *Int. J. Clin. Pharmacol. Ther.* **2000**, *38*, 111 – 121.
[14] Attempts to determine the activities of the precursors **3a–c**, which contain ester groups, failed due to insufficient solubility in the assay system.
[15] A. Hilgeroth, M. Wiese, A. Billich, *J. Med. Chem.* **1999**, *42*, 4729 – 4732.
[16] Assay with 3-(4,5-dimethylthiazol-2-yl)-2,5-diphenyltetrazolium bromide (MTT) as substrate: S. N. Pandeya, D. Sriram, E. De Clercq, C. Pannecouque, M. Witvrouw, *Indian J. Pharm. Sci.* **1998**, *60*, 207 – 212.

Fluorescence Spectroscopic Quantification of the Release of Cyclic Nucleotides from Photocleavable [Bis(carboxymethoxy)coumarin-4-yl]methyl Esters inside Cells**

Volker Hagen,* Stephan Frings, Jürgen Bendig, Dorothea Lorenz, Burkhard Wiesner, and U. Benjamin Kaupp

Caged compounds are an elegant means to produce rapid jumps in the concentration of chemical messenger molecules inside cells.[1] Caged compounds are photolabile inactive derivates of biologically active molecules. The biologically active substance is rapidly released by a photochemical reaction. Caged compounds allow the elucidation of complex intracellular processes and their resolution in time and space.

For many applications it would be useful to determine quantitatively the degree of photolysis of the caged compound inside cells. In a few cases this has been possible by a rather complicated calibration of the cellular reaction. Here we show that the determination of the amount of released cyclic nucleotides is feasible by fluorescence measurements, using the axial and equatorial diastereomers of [6,7-bis(carboxymethoxy)coumarin-4-yl]methyl (BCMCM) esters of cyclic adenosine-3′,5′-monophosphate (cAMP) **1** and cyclic guanosine-3′,5′-monophosphate (cGMP) **2**,[2] which are excellent phototriggers for cyclic nucleotides.

Upon irradiation with UV light in aqueous buffer solution and inside cells, **1** and **2** rapidly produce (within 2–5 ns) cAMP

[*] Dr. V. Hagen, Dr. D. Lorenz, Dr. B. Wiesner
Forschungsinstitut für Molekulare Pharmakologie
Robert-Rössle-Strasse 10, 13125 Berlin (Germany)
Fax: (+49) 30-94793-159
E-mail: hagen@fmp-berlin.de
Priv.-Doz. Dr. S. Frings, Prof. Dr. U. B. Kaupp
Institut für Biologische Informationsverarbeitung,
Forschungszentrum Jülich (Germany)
Doz. Dr. J. Bendig
Institut für Chemie
Humboldt-Universität Berlin (Germany)

[**] This work was supported by the Deutsche Forschungsgemeinschaft and the Fonds der Chemischen Industrie. We thank B. Dekowski und Dr. S. Helm for technical assistance.

  0044-8249/02/4119-3625 $ 20.00+.50/0

and cGMP, respectively [3] and 6,7-bis(carboxymethoxy)-4-(hydroxymethyl)coumarin (**3**, BCMCM-OH) (Scheme 1). The photolysis proceeds free of competing side reactions with quantum yields of 0.08–0.14.[2] Per molecule of **3**, one molecule of either cAMP or cGMP is produced.

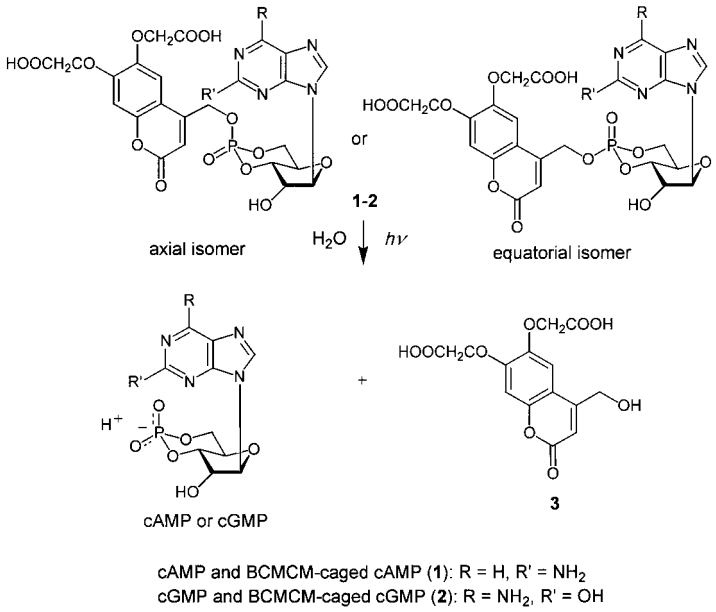

Scheme 1. Photolysis of **1** and **2**.

The fluorescence quantum yields of **1** and **2** are small, whereas the alcohol **3** is strongly fluorescent (Table 1, see also Figure 1 a). Therefore, upon photolysis of the caged compounds, the fluorescence is strongly enhanced (in aqueous buffer 40- to 50-fold increase) (Figure 1 b). In HEPES buffer (HEPES = 2-[4-(2-hydroxyethyl)-1-piperazinyl]ethansulfonic acid), the relationship between the degree of photolysis and the increase in fluorescence is linear for all BCMCM-caged cyclic nucleotides. This correlation is shown for the equatorial isomers of **1** and **2** in Figure 2. Therefore, it is feasible to determine the concentration of released **3** and thereby also the concentration of cAMP and cGMP under these conditions.

Table 1. Fluorescence maxima λ_f^{max}, fluorescence quantum yields φ_f and fluorescence life times τ_f of the BCMCM-caged cAMPs and cGMPs **1**–**2**, as well as of **3** in HEPES–KOH buffer, pH 7.2; $\lambda_{exc} = 333$ nm.

Compound	λ_f^{max} [nm]	φ_f[a]	τ_f [ns]
1 (axial)	440	0.015	n.d.
1 (equatorial)	439	0.016	< 0.2
2 (axial)	436	0.012	n.d.
2 (equatorial)	441	0.014	< 0.2
3	431	0.62	3.18

[a] Error limit ± 0.002 (**1**,**2**) and ± 0.01 (**3**); n.d. = not determined.

The fluorescence of **1**, **2**, and **3** in cells is similar to that of the respective substances in aqueous solutions, that is, **3**, which has been introduced into HEK293 cells by using a micropipette, is strongly fluorescent (Figure 3), in contrast to 7-

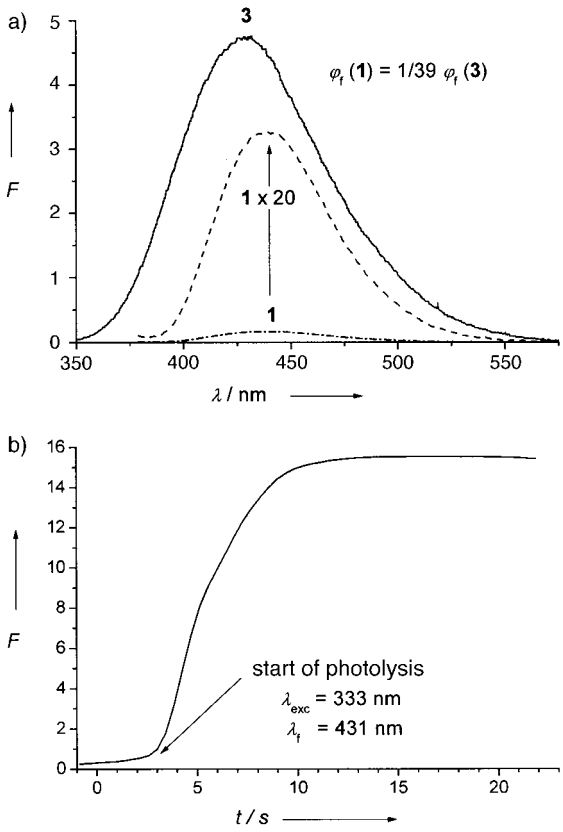

Figure 1. a) Fluorescence spectra of 50 μM solutions of the equatorial isomer of **1** and of **3**. F = relative fluorescence intensity; b) increase in fluorescence of a 50 μM solution of the equatorial isomer of **1** as a function of the irradiation time; solutions in HEPES–KOH buffer, pH 7.2.

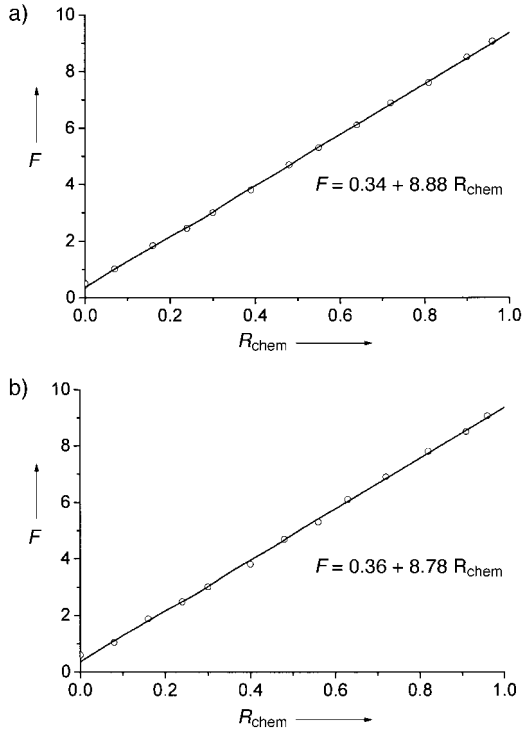

Figure 2. Correlation between the enhancement of the relative fluorescence and the extent of photolysis (R_{chem}) of 50 μM solutions of the equatorial isomers of **1** (a) and **2** (b) in HEPES-KOH buffer, pH 7.2.

  0044-8249/02/4119-3626 $ 20.00+.50/0

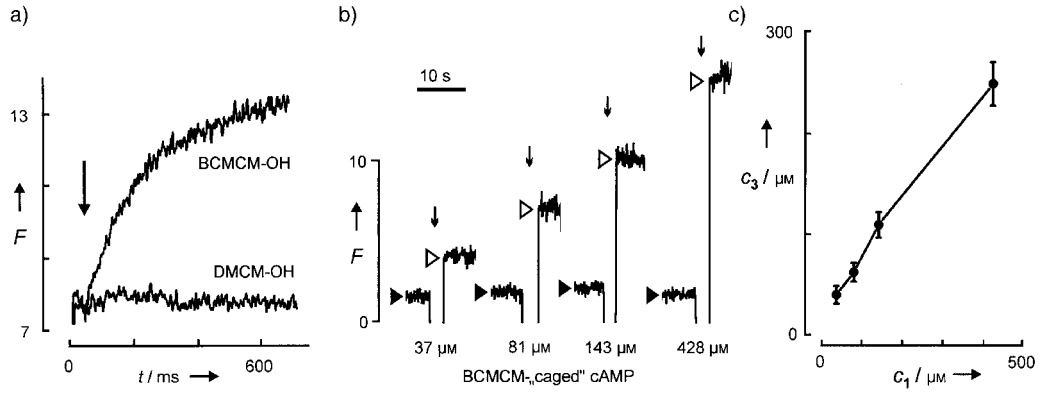

Figure 3. Determination of the photolytically liberated concentration of **3** in HEK293 cells: a) visualization of cell loading with 100 μM BCMCM-OH (**3**) or DCMCM-OH through the patch pipette by monitoring the fluorescence intensity (excitation: 340 nm, emission >420 nm, scaling in counts ms^{-1}). Fluorescence intensity increases with the concentration of **3**; b) determination of the concentration of **3** following photolysis of **1** in four HEK293 cells which were loaded with the indicated concentration of **1** as well as with 35 μM **3** as standard for the calibration of intracellular fluorescence. The fluorescence intensity used for calibration (F_C, filled arrowhead) was measured after subtraction of background light. Following illumination (arrows, $t=2$ s, $\lambda=365$ nm), the fluoresence intensity increases to the value F_1 (open arrowheads). The calculated concentration of liberated **3** [$c=(F_1-F_C)/F_C 35$ μM] was 49 μM, 96 μM, 148 μM, and 271 μM, respectively; c) concentration of photolytically liberated intracellular **3** plotted against the concentration of **1** in the pipette solution (illumination: $t=2$ s, $\lambda=365$ nm). Mean values ± SD obtained from five cells per concentration value. c_1 = concentration of **1**, c_3 = concentration of liberated **3**.

methoxy-[4] and 6,7-dimethoxy-4-(hydroxymethyl)coumarin (DMCM-OH),[5] whose fluorescence is totally quenched inside HEK293 cells.[6] This result indicates that the hydrophilic carboxymethoxy groups in **3** inhibit the quenching of fluorescence by cellular constituents. Therefore, flash photolysis of BCMCM-caged cyclic nucleotides results in a concentration-dependent increase of fluorescence inside cells, as shown in Figure 3b for compound **1**. The concentrations of **3** and thereby that of cAMP, determined by the light-induced fluorescence enhancement, increase almost linearly with the concentration of photolyzed **1** (Figure 3c).

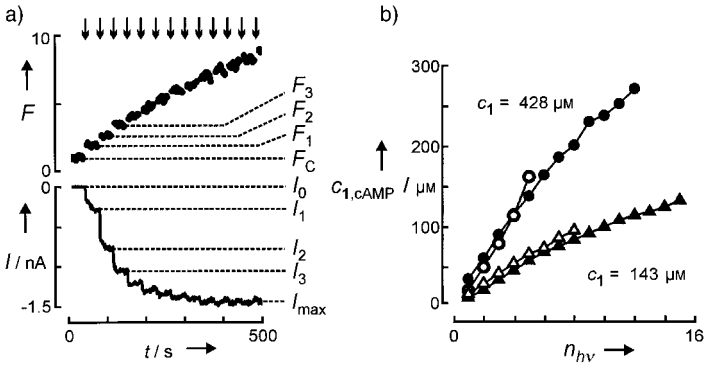

Figure 4. Quantification of the concentrations of **3** and cAMP following photolysis of **1**: a) a HEK293 cell transfected with DNA encoding CNGA 2 channels was loaded with 428 μM **1** as well as with 35 μM **3** for internal calibration. The fluorescence recording (upper trace) shows liberation of **3** during a series of UV flashes ($t=20$ ms, $\lambda=365$ nm). The simultaneous current recording (lower trace) shows activation of the CNGA2 channels by photoreleased cAMP. Both fluorescence intensity and current amplitude can be used to calculate photolysis; b) calculation of photolytic liberation of **3** from the increase of fluorescence intensity (see Figure 3), and calculation of cAMP liberation from the relative current $I_{rel}=I/I_{max}$ using the Hill equation.[9] The results for quantification of photolysis obtained from fluorescence measurements (▲●) and from analysis of current recordings (△○) are in good agreement. While the current calibration is limited by the maximal channel activation at roughly 150 μM cAMP, the fluorescence-based calibration can be extended to higher concentrations. I = current; n = number of flashes; $c_{1,cAMP}$ = concentration of photoreleased cAMP.

Figure 4a shows the light-induced increase in intracellular fluorescence and the cAMP-induced current in cells loaded with **1** and expressing the cAMP-gated ion channel of olfactory neurons (CNGA2). Each flash of light incrementally increases both the fluorescence and the current. The concentration of released **3**, which corresponds to the concentration of released cAMP, can be determined from the fractional change in fluorescence (Figure 3). The obtained concentration of released cAMP agrees very well with that independently determined from the incremental increase of open CNGA2 channels[7] (Figure 4b). Similar results were obtained for the release of cGMP from **2** and the release of 8-substituted cyclic nucleotides from the respective BCMCM-caged derivatives. These experiments demonstrate that it is feasible to follow the release of cyclic nucleotides from BCMCM-caged cyclic nucleotides quantitatively by fluorescence measurements. We expect that these measurements can be extended to other BCMCM-caged derivatives, provided their fluorescence is distinctly different from that of the photolysis products.

This technique allows, for the first time, the quantitative dose–response relations of cellular reactions triggered by cyclic nucleotides to be established. Recently it was reported[8] that adenylyl cyclases, which synthesize cAMP, and cAMP-gated channels, appear to colocalize to a subcompartment of a cell line and that diffusional exchange between this compartment and the cytosol is restricted. We did not observe a difference in the concentrations of cytosolic cAMP reported by the fluorescence signal and the "local" cAMP concentration in the vicinity of the CNGA2 channel. The methods described here will allow the hypothesis of cellular subcompartments, in which the diffusion of intracellular messengers is restricted in more quantitative terms, to be tested.

Received: April 10, 2002 [Z19070]

  0044-8249/02/4119-3627 $ 20.00+.50/0

[1] A. M. Gurney, H. A. Lester, *Physiol. Rev.* **1987**, *67*, 583 – 617; "Photochemical Probes in Biochemistry": J. F. Wooton, D. R. Trentham, *NATO ASI Ser. C* **1989**, *272*, 277 – 296; J. P. Y. Kao, S. R. Adams, *Optical Microscopy: Emerging Methods and Applications*, Academic Press, San Diego, **1993**, S. 27 – 85; S. R. Adams, R. Y. Tsien, *Annu. Rev. Physiol.* **1993**, *55*, 755 – 784; J. E. T. Corrie, D. R. Trentham, *Bioorganic Photochemistry: Biological Applications of Photochemical Switches*, Wiley, Chichester, **1993**, S. 243 – 305; G. P. Hess, *Biochemistry* **1993**, *32*, 989 – 1000; Ed. G. Marriott, *Methods Enzymol.* **1998**, *291*.
[2] V. Hagen, J. Bendig, S. Frings, T. Eckardt, S. Helm, D. Reuter, U. B. Kaupp, *Angew. Chem.* **2001**, *113*, 1078 – 1080; *Angew. Chem. Int. Ed.* **2001**, *40*, 1046 – 1048.
[3] J. Bendig, S. Helm, R. Schmidt, C. Schweitzer, V. Hagen, unpublished results..
[4] J. M. Sehgal, T. R. Seshadri, *J. Sci. Ind. Res.* **1953**, *12B*, 346 – 349.
[5] T. Eckardt, V. Hagen, B. Schade, J. Bendig, *J. Org. Chem.* **2002**, *67*, 703 – 710.
[6] V. Hagen, J. Bendig, S. Frings, B. Wiesner, B. Schade, S. Helm, D. Lorenz, U. B. Kaupp, *J. Photochem. Photobiol. B* **1999**, *42*, 91 – 102.
[7] V. Hagen, C. Dzeja, S. Frings, J. Bendig, E. Krause, U. B. Kaupp, *Biochemistry* **1996**, *35*, 7762 – 7771.
[8] T. R. Rich, K. A. Fagan, H. Nakata, J. Schaack, D. M. F. Cooper, J. W. Karpen, *J. Gen. Physiol.* **2000**, *116*, 147 – 161.
[9] Hill equation: I_{max} is the current at maximal channel activation, $K_{1/2}$ is

$$c_{cAMP} = K_{1/2} \cdot \sqrt[n]{\frac{I_{rel}}{1 - I_{rel}}}$$

the cAMP concentration that gives half-maximal channel activation (45 μM),[9] and n is the Hill coefficient (1.8). W. Bönigk, J. Bradley, F. Sesti, F. Müller, I. Boekhoff, G. V. Ronnett, U. B. Kaupp, S. Frings, *J. Neurosci.* **1999**, *19*, 5332 – 5347.

Protonated Benzene: IR Spectrum and Structure of $C_6H_7^+$**

Nicola Solcà and Otto Dopfer*

The protonation of aromatic molecules is a central process to organic chemistry. For example, protonated aromatic molecules (AH^+) occur as intermediates in electrophilic aromatic substitution reactions, probably the most characteristic reaction mechanism for aromatic molecules.[1] Spectroscopic studies in solution reveal that fundamental properties of these ion–molecule reactions depend strongly on the environment.[1,2] To separate solvation effects from intrinsic molecular properties, gas-phase studies are required.[3] However, to date, nearly all data about gas-phase protonation processes have come from mass spectrometric methods,[3] which provide only indirect and often inconclusive structural information. Spectroscopic data for direct and unambiguous structural characterization have not been reported for any isolated AH^+ ion, mainly because of the difficulties encountered in producing a large abundance of these species. Gas-phase spectra of AH^+ are desirable, not only to investigate fundamental reaction mechanisms, but also to identify these ions in terrestrial and extraterrestrial hydrocarbon plasmas, such as combustion flames[4] and interstellar media.[5]

Protonated benzene, $C_6H_7^+$, is the simplest protonated aromatic hydrocarbon and for more than half a century has served as a benchmark for investigating the mechanism of electrophilic aromatic substitutions. Most quantum chemical studies consider three binding sites for the proton to the benzene molecule (Figure 1).[6] The benzenium ion (**1**), often

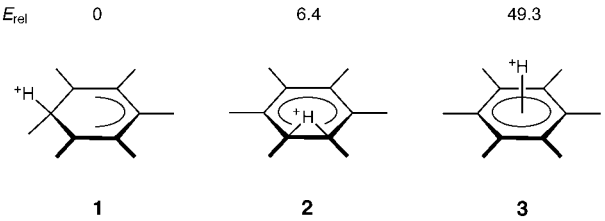

Figure 1. Calculated structures and relative energies (E_{rel} in kcal mol^{-1}) of stationary points on the potential energy surface of $C_6H_7^+$:[14] **1**: σ complex (benzenium ion, Wheland intermediate, global minimum, C_{2v} symmetry); **2**: bridged structure (benzonium ion, first-order transition state, C_s symmetry); **3**: π complex (second-order transition state, C_{6v} symmetry).

called the σ complex or Wheland intermediate, is the global minimum on the calculated $C_6H_7^+$ potential. The bridged structure **2** is predicted to be the lowest transition state for proton migration between equivalent σ complexes, with an activation barrier of $E_a \approx 6$–11 kcal mol^{-1}. The face-protonated π complex **3** is identified as a second-order transition state which lies ≈ 50 kcal mol^{-1} above **1**. Apart from **1**–**3**, several other less stable $C_6H_7^+$ isomers exist.[7] These isomers are not considered further, as they do not have a six-membered ring and are thus not created in the present experimental procedure.[3a,7,8]

Spectroscopic evidence for a σ complex of $C_6H_7^+$ in the condensed phase comes from NMR,[9] IR,[9b,d,10] and UV spectroscopy,[10] and X-ray crystallography[9e] of either salts or superacid solutions. The low-temperature NMR spectra are consistent with a static σ complex **1**, whereas spectra recorded at higher temperatures indicate the equivalence of all protons, which is caused by rapid intramolecular exchange.[9a] The derived activation barrier for proton migration, $E_a = 10 \pm 1$ kcal mol^{-1},[9a] is consistent with the theoretical values,[6] assuming that **2** is the lowest transition state for the intramolecular 1,2-proton transfer. The conclusions drawn from gas-phase studies to ascertain the $C_6H_7^+$ structure without interference from strong solvation effects are controversial. The UV spectrum of isolated $C_6H_7^+$[11] indeed deviates significantly from the solution spectrum[10] and contains no conclusive structural information. Structure determination by mass spectrometry[3,7] suffers from indirect and disputable interpretations.[3a] Although most studies infer that **1** is the most stable $C_6H_7^+$ structure,[3a–d] a recent analysis[3e] leads to the conclusion that **3** is probably lower in energy by ≈ 3–4 kcal mol^{-1}.

[*] Priv.-Doz. Dr. O. Dopfer, Dipl.-Chem. N. Solcà
Institut für Physikalische Chemie
Universität Basel
Klingelbergstrasse 80, 4056 Basel (Switzerland)
Fax: (+41) 61-267-3855
E-mail: otto.dopfer@unibas.ch

[**] This study is part of project no. 20-63459.00 of the Swiss National Science Foundation. O.D. is supported by the Deutsche Forschungsgemeinschaft by a Heisenberg Fellowship (DO 729/1-1).

  0044-8249/02/4119-3628 $ 20.00+.50/0